Ethoxysalicylaldehyde S-Allylisothiosemicarbazone Schiff Base Metal Complexes: Synthesis, Spectroscopic Characterization, Biological Studies, Molecular Docking and Drug-Likeness Analysis

M. Sridhar[1,2], Ajmeera Ramesh[3], Revathy Sundara Moorthy[4], P. Muralidhar Reddy[4], K. Laxma Reddy[4]*, Krishnam Raju Atcha[1*]

[1] *Department of Chemistry, University College of Technology Osmania University, Hyderabad-500007*
[2] *Department of Chemistry, SRR Govt. Arts & Science College, Karimnagar-505001*
[3]*Department of Chemistry, NIT Warangal-506004*
[4] *Department of Chemistry, University College of Science Osmania University, Hyderabad-500007*
E-mail: klreddy200542@gmail.com, krishnamrajua@osmania.ac.in
doi: 10.48047/ecb/2023.12.si4.1184

ABSTRACT- 3-Ethoxysalicylaldehyde S-allylisothiosemicarbazone hydrobromide, **HL** a new tridentate Schiff base and its cationic complexes of Co[1], Ni[1], Cu[1] and Zn[1] were successfully prepared. The typical formulae for complexes are [**$Co(L)_2$](1), [$Ni(L)_2$](2), [$Cu(L)_2$](3)** and **[$Zn(L)_2$](4)**. The prepared complex analogues have been characterized with instruments such as infrared, ^{1}H NMR, ^{13}C NMR, elemental analysis, electronic and fluorescence spectroscopic studies. The physicochemical results showed that the Schiff base (**HL**) coordinates the NNO donor set to form tridentate to the central metal ions. Although complexes of the **HL** ligand exhibited significant fluorescence intensity. The synthesized compounds have been tested against bacterial pathogens. Compared to the reference antibiotic drug, streptomycin, the **[$Zn(L)_2$]** complex was very effective against both microorganisms in the zone of inhibition ranges (22–27 mm) and (28–30 mm). Additionally, the anti-diabetic qualities were also looked into. When compared to the reference drug acarbose, which has an IC_{50} = 33.17 ± 2.39 µm, the **[$Cu(L)_2$]** and **[$Zn(L)_2$]** complexes have inhibitory potential against α-amylase with significant inhibition of IC_{50} = 28.37 ± 2.17 and 29.53 ± 2.08 µm. The desired ligand-protein interactions with the active site residues were suggested by the molecular docking studies. Whereas the **[$Ni(L)_2$]** and **[$Zn(L)_2$]** complex shown well-oriented interaction conformations with a -6.5 kcal/mol for E. coli (PDBID: HNJ) protein active site. Hydrogen, hydrophobic, and electrostatic bonds interactions were also generated by some of these complexes. *In-silico* analysis of the ADME properties of the bioactive **HL** ligand have been shown that drug-likeness property.

KEYWORDS-Isothiosemicarbazone. Metal complexes. Antibacterial. Antidiabetic properties. *In-silico* docking. ADME Investigations

1. INTRODUCTION

Thiosemicarbazide reacts with alkyl halides to make isothiosemicarbazides, which can combine with aldehydes and ketones to make isothiosemicarbazones[2-4]. Jensen *et al*. synthesized complexes of palladium, nickel, cobalt, and iron using thiosemicarbazide[5, 6]. Isothioamidic nitrogen functions as a better donor whenever sulfur has been alkylated[7, 8]. Modern synthetic organic chemistry uses functionalized allylic bromides, which are adaptable building blocks produced through the Morita-Baylis-Hillman (MBH) reaction [3]. Allylic bromides are excellent substrates for nucleophilic displacement with a variety of C-, O-, N-, P-, S-, and Se-nucleophiles due to their highly electrophilic nature and simple procedures for synthesis[7, 9]. Typically, through nitrogen atoms of isothioamide, azomethine and similar donor hetero atoms such as oxygen/sulphur the coordination of tridentate isothiosemicarbazides to metal is done. Tridentate

isothiosemicarbazone complexes had a variety of their structures determined [10-12]. In complexes, isothiosemicarbazides or their derivatives generally exhibit biological activity, including antimicrobial, antituberculosis, antileukemia, antibacterial, and antifungal characteristics as well as antidiabetic capabilities(Bal, 2007 #19;Belicchi-Ferrari, 2005 #21;Cocco, 2002 #17;De Logu, 2005 #18;Plumitallo, 2004 #16;Yanardag, 2009 #20). Depending on the kind of functional moieties/different metal centres are employed to synthesize them, isothiosemicarbazones biological activity will alter[13, 14]. Copper sites offer antibacterial, antifungal, and anticancer effects as it damages the respiratory chain of microbes within short time [15]. Hence, Copper complexes are preferred.

The current study on the synthesis of 3-ethoxysalicylaldehyde S-allylisothiosemicarbazone hydrobromides, **HL** (**Scheme 1**) and its cationic complexes of Co [1], Ni [1], Cu [1], and Zn [1] complexes along with their characterizations are reported. The characterization of these compounds was done by spectral investigations and their biological properties has also been studied.

2. EXPERIMENTAL

2.1 MATERIALS AND PHYSICAL MEASUREMENTS

None of the solvents and reagents used were purified before usage; they were all obtained from commercial sources and analytical grades. Themo Finnigans Flash Elemental Analyzer 1112EA has been used to execute elemental analysis for elements like C, H, N and S. FTIR spectra in the 400–4000 cm^{-1} range were collected using a Perkin Elmer Model 100S Spectrophotometer. Bruker Ascend ^{1}H-400 and ^{13}C-100 MHz NMR spectrometer were used to acquire the spectra. A Shimadzu Model UV-1800 UV-Spectrophotometer (200–1100nm) was opted to get electronic spectra in DMSO. A PerkinElmer LS55 fluorescence spectrometer was used to measure fluorescence. The Stuart SNP-30, a melting point apparatus was opted to determine the melting points.

2.1.1 Synthesis of 3-ethoxysalicylaldehyde S-allylisothiosemicarbazone hydrobromide (HL)

Dissolving of thiosemicarbazide (0.273 g, 3mmol) was done in about 15ml ethanol and added allyl bromide (0.386 g, 3 mmol), stirred and refluxed for 10 minutes at 90 °C on a magnetic stirrer. The resultant solution was then blended with 3-ethoxysalicylaldehyde (0.498 g, 3 mmol), and the reflux was maintained for a further 2–4 hours. Filtration then separated an yellow precipitate (**Scheme 1**)that has to be washed several times using cold EtOH and then dried at room temperature. Color: Yellow. Yield: 1.8g, 76.5%. M.P.: 248 °C.

Calcd. Found % for (**HL**), $C_{13}H_{18}BrN_3O_2S$: C, 43.34; H, 5.04; N, 11.66; S, 8.90. Found: C, 43.32; H, 5.01; N, 11.61; S, 8.89%. IR (KBr) cm^{-1}: ν(OH) 3400, ν(N-H) 3318, ν(C=N-)1593 m, 1604 s, ν(C=C) 1442 m, ν(C-O) 1246 m, ν(N-N) 1098 m, ν(C-S)736 s. UV/Vis (DMSO) λ_{max} [16]: 295, 350. ^{1}H-NMR(400 MHz, DMSO-d_6): δ=13.1 (b, HBr), 9.4 (s, 1H, OH), 9.6 (s, 2H, N15H), 8.7 (s, 1H, C7H), 7.6(d,1H,C6H), 7.0(dd, 1H, C2H), 6.8(d, 1H,C1H), 5.8-5.9(m,1H,C18H), 5.2-5.4(m, 2H, C19H), 4.0 (d, 2H, C17H), 4.1(m,2H,C10H), 1.35-1.38 (t,3H, C11H), ^{13}C-NMR (100 MHz, DMSO-d_6):δ163.2, 149.9, 147.9, 147.5, 131.5, 120.5, 119.9, 119.3, 118.8, 116.2, 64.7, 34.1, 14.9, (ESI–MS (m/z): Calc.: 359.03: Found: 360.05 $[M+H]^+$.

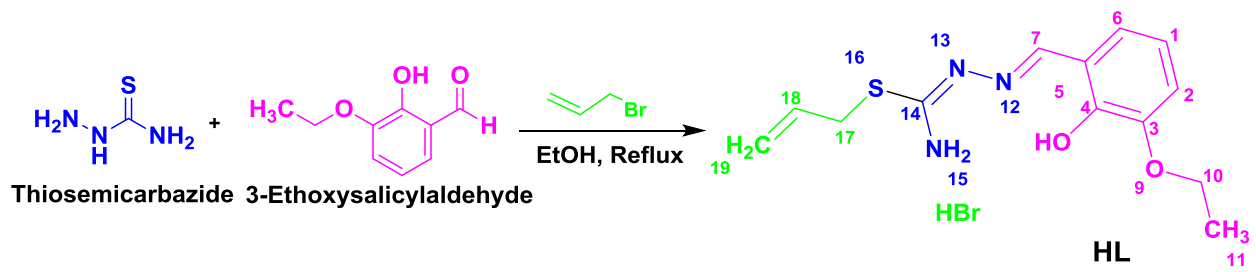

Scheme 1. Schematic synthesis of 3-Ethoxysalicylaldehyde S-allylisothiosemicarbazone hydrobromide **(HL)**

2.1.2 Synthesis of bivalent metal complexes (1-4)

Complexes Co [1], Ni [1], Cu [1], and Zn [1] complexes i.e., from **(1-4)** were synthesized using metal acetates. A double molar amount of **HL** (0.07g, 0.20 mmol) was added to this hot ethanol solution drop by drop while it was being stirred constantly for 4–6 hours. Triethylamine was used for proton abstraction from **HL**. The resulting solution has been filtered, washed with EtOH, followed by air drying and made to stand overnight, yielding a respective colour compound as depicted in **Scheme 2**.

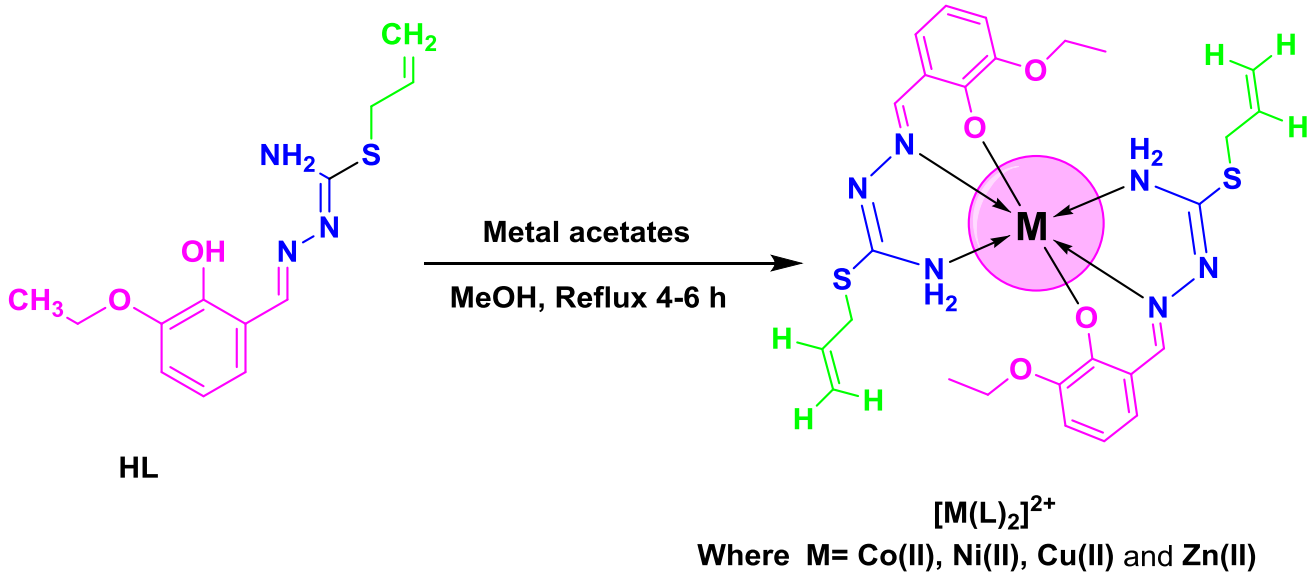

Scheme 2. Schematic synthesis representation of complexes (**1-4**)

[Co(L)$_2$] (1): Dark green. Yield: 62.0%.M.P.: >289 °C. Anal. Calcd. for $C_{26}H_{32}CoN_6O_4S_2$: C, 50.73; H, 5.24; N, 13.65; S, 10.42. Found: C 50.71; H, 5.22; N, 13.65; S, 10.40%. IR (KBr) cm^{-1}: ν(N-H) 3252 s, ν(C=N) 1592 m, ν(C=C) 1474 m, ν(C-O) 1242 m, ν(N-N) 1089 m, (C-S) 739 w, (Co-O) 573 m; (Co-N) 475 m. UV-Vis (DMSO) λ_{max} [16]: 296, 421.
[Ni(L)$_2$] (2): Brick red: Yield: 65.0%. M.P.: >329 °C. Anal. Calcd. for $C_{26}H_{32}N_6NiO_4S_2$: C, 50.75; H, 5.24; N, 13.66; S, 10.42. Found: C, 50.70; H, 5.23; N, 13.66; S, 10.41%. IR (KBr) cm^{-1}: ν(N-H) 3398 s, ν(C=N) 1595 m, ν(C=C) 1441 m, ν(C-O) 1249 m, ν(N-N) 1096 m, (C-S) 734 w, (Ni-O) 560 m; (Ni-N) 469 m. UV-Vis (DMSO) λ_{max}, [16]: 305, 400, 485.
[Cu(L)$_2$] (3): Red: Yield: 60.0%. M.P.: >325 °C. Anal. Calcd. for $C_{26}H_{32}CuN_6O_4S_2$: C, 50.65; H, 5.20; N, 13.55; S, 10.34. Found: C, 50.65; H, 5.19; N, 13.48; S, 10.32%. IR (KBr) cm^{-1}: ν(N-H) 3397 s, ν(C=N) 1602 m, ν(C=C) 1439 m, ν(C-O) 1244 m, ν(N-N) 1085 m, (C-S) 734 w, (Cu-O) 592 m; (Cu-N) 499 m. UV-Vis (DMSO) λ_{max}, [16]: 324, 400, 489.
[Zn(L)$_2$] (4): Orange: Yield: 76.3%. M.P.: >336 °C. Anal. Calcd. for $C_{26}H_{32}N_6O_4S_2Zn$: C, 50.20; H, 5.19; N, 13.51; S, 10.31. Found: C, 50.19; H, 5.17; N, 13.49; S, 10.30%. IR (KBr) cm^{-1}: ν(N-H) 3318 s, ν(C=N) 1604 m, ν(C=C) 1442 m, ν(C-O) 1246 m, ν(N-N) 1098 m, (C-S) 736 w, (Zn-O) 604 m; (Zn-N) 526 m. UV-Vis (DMSO) λ_{max}[16]: 326, 360, 460.

2.2 In-vitro antibacterial activity

The ligand, **HL** and its complexes (**1-4**) biological activities were tested using the agar disk diffusion method [17, 18]. To assess their antibacterial effectiveness against selected pathogenic bacterial species, Viz., Gram-positive - Escherichia coli, *Salmonella paratyphi*, and Gram negative - *Bacillus subtilis*, *Staphylococcus aurous*. The experiments are repeated three times under the same circumstances. After 24

hrs incubation at 37℃, the plates were measured for Zone of Inhibition (ZoI). The outcomes were contrasted with those of streptomycin, a widely used antibiotic drug.

2.3 Alpha-Amylase inhibition assay method

A previously reported approach [19, 20] was used to test the compounds ability to inhibit α-amylase, with a few minor modifications. In brief, a 1.5 mL sample tube was filled with test inhibitor of about 40 µL solution and α- amylase solution of about 40 µL, which at room temperature was incubated for 10 min in a buffer of 0.02 M which are then at pH 6.9 was incubated for about 10 min in a 0.02M sodium phosphate buffer with 0.006M sodium chloride at ambient temperature. The pre-incubated tubes were then filled with starch solution of about 40 µL dissolved in 1% DMSO and the mixture was incubated at 25 °C for an additional 10 minutes. Following the addition of DNSA as coloring agent for about 100 µL agent (10g Sodium potassium tartrate, a gram of 3,5-dinitrosalicylic acid and 2N sodium hydroxide for about 20 ml was made upto 100 ml using distilled water) the solution in a boiling water bath was incubated for 5 minutes. As at room temperature the reaction mixture cools, add to it the distilled water to make 500 µL.

2.4 ADMET drug predictions

Computational techniques have been playing a significant part in process of drug design. There is a decrease found in the experimental number while an increase in the success rate. The pharmacokinetic properties of ligands such as ADMET (Absorption, Distribution, Metabolism, Excretion and Toxicity) are investigated to confirm their function in the human body. In silico prediction refers to the similarity between studied compounds and drugs. For subject ligands, these pharmacokinetic parameters were evaluated to determine their potential as drug candidates. The ADMET properties of the ligands were evaluated by the Swiss ADME system [21]. Drug-like properties of ligands were predicted using Lipinski's rule of five. The pharmaceutical industry frequently and effectively uses the Lipinski Rule of Five to select the best molecule for a drug. Consequently, the bioavailability of ligand can be predicted by determining their physicochemical properties [22]. Therefore, if a ligand meets the following criteria: where molecular weight should be less than 500, the number of H-bond acceptors should be lower than 10, the number of H-bond donors should be lower than 5 and the lipophilicity log P should be below 5 is expressed it is like a drug. Therefore, if the properties of a molecule fall outside these limits, it is unlikely to be bioavailable when taken orally as a drug.

2.5 Docking studies

To establish the therapeutic activity of **HL** and its $\mathbf{[M(L)_2]^{2+}}$, ChemSoft Chem Draw Ultra 12.0 software was used to draw ligand structure and compounds listed against the 1HNJ protein were docked. The letter 1HNJ indicates the *E. coli FabH-CoA* complex. *FabH* receptor was opted as a target to evaluate the antibacterial activity of natural compounds and *FabH* plays a role in bio-synthesis of fatty acid[23]. The 3D structure of target protein receptors were taken from protein database (http://www.rcsb.org) [22]. The compounds studied were used as substrates. Each compound was optimized for substrate preparation by energy minimization, then a new database was created and stored in PDB format. Addition of hydrogen atoms, pairing of acceptor species, adjustment of potential energy, elimination of water molecules and further the search for active pockets and creation of dummies were used to construct the target acceptor. The interaction parameters and docking patterns were taken for analysis of interaction properties and rate inhibition activity depends on a scoring function (S, kcal/mol)[24]. To analyze molecular docking, AutoDockVina (Ver.1.5.6) and Discovery Studio (Ver. 2021) programs were used.

3. RESULTS AND DISCUSSION

This section includes physical and analytical data of the newly synthesized Schiff base ligand, -ethoxysalicylaldehyde, S-allylisothiosemicarbazone hydrobromide, **HL** along with its four new coordinated ions i.e., Co [1], Ni [1], Cu [1], and Zn [1]. Thiosemicarbazide was S-alkylated with alyl bromide and S-allylisothiosemicarbazone hydrobromide was condensed with 3-ethoxysalicylaldehyde to gain good yield of the product as in (**Scheme 1**). By directly reacting **HL** with tridentate NNO donors and a set of

thiosemicarbazide, 3-ethoxysalicylaldehyde and respective metal salts. The compounds are then suspended in air and their physical and analytical results were observed to be consistent in regard to the molecular formula.

In DMF solution, the conductivity of the prepared complexes was measured. The molar conductivities 10^{-3} M of the complexes (**1-4**) ranges from 9.50-19.03 μS at ambient temperature, indicating their non-electrolyte character[18] and the absence of ions beyond the coordination sphere [25].

3.1 Spectral studies

3.1.1 FTIR study

To understand the metal ion coordination, the comparison of major IR bands of ligand, **HL** and its complexes, **1-4** were done.

The broad bands at 3273 cm^{-1} in the ligand, **HL** relates to the ν(OH) [8]. This band disappears after complexation, conforming that coordination occurs via phenolic oxygen[26], while the bands at 3078 and 2978 $cm^{-}1$ [8] are corresponding to $15NH_2$ symmetric and assymetric vibrations, respectively. After coordination, these peaks change to lower and higher frequencies [27]. At 3400 cm^{-1}, in IR spectra of the complexes, a new band was noticed for ν[28]. The free HL, azomethine and isothioamide absorption together assigned to ν(NH_2) and ν(N_{13}=HC_{14}) was noticed at 1631 and 1581 cm^{-1} correspondingly[29]. An intense band at 1603cm^{-1} was due to aryl-C7=N12-N13 stretching vibration. C=C absorptions were observed between 1450 and 1600 cm^{-1}. In free HL, the phenolic C-O band observed at 1258 cm^{-1} shifts after co-ordination to lower frequency and the deformation band of phenolic O-H at 1408 cm^{-1} is absent that confirms co-ordination of ligand to metal ions via phenolic oxygen[30]. While in the free HL spectrum, the Co [1], Ni [1], Cu [1] and Zn [1] complexes showed stretching vibrations of (N-N) at 1098 cm^{-1} that shifted to lower frequency on co-ordination. Additionally, the peak C-S w band at 734-739 cm^{-1} is indicative of S-alkylation[31]. The above observation was supported by the formation of two weak bands in all metal complexes in the regions 469–526 cm^{-1} and 560–604 cm^{-1} bands attributed to ν(M-N) and (M-O) [30].

3.1.2 UV-Vis study

The electronic spectra of **HL** and its four complexes recorded in DMSO solvent. Ligand, **HL** found two bands around 240 and 400 nm. The first bands at 295 nm are attributed to the π→π* transitions of the aromatic ring, the azomethineic group and the isothioamidic group of the ligand, respectively [32]. The other band at 350 nm corresponds to n→π* transitions of azomethinic and isothioamidic group, respectively [33, 34]. Due to the π→π* transitions and a broad absorption band at 460 nm, **$[Zn(L)_2]$ (4)** underwent a blue shift at 326-500 nm **Figure 2** upon free ligand, **HL** complexation. In spectra **(1)**, **(2)** and **(3)**, the azomethine and isothioamide chromophore π→π* transitions are seen at 296, 305, and 324 nm, respectively. N→M and O→M charge transfer transitions can be assigned a band located at 421 nm for **(1)**, 400 and 485 nm for **(2)** and 400 and 489 nm for **(3)**. The rationale for these shifts is the variation in electron density and subsequent coordination. Although having n orbitals, these after complexation are more stable. The complex spectra exhibit LMCT charge transfer bands. Whereas there are no d-d transitions noticed in any of the complexes that are shielded by charge transfer and intra ligand transition bands.

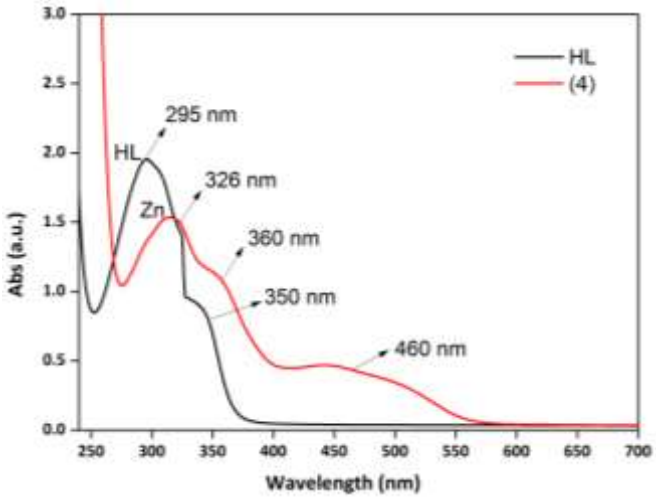

Figure 2. UV-Vis spectra of ligand —**HL** and its complex —**Zn[1] (4)**

3.1.3 Fluorescence study

In coordination chemistry, the steady-state fluorescence spectral investigations provide further proof for coordination between **HL** and its $\mathbf{[M(L)_2]^{2+}}$ recorded at room temperature. The Schiff base fluorescence excitation spectrum, **HL** and its corresponding metal complexes' transitions were measured as an excitation wavelength at 274 nm using DMSO solvent in ($2x10^{-4}$ M) are shown in **Figure 3**. It is noticed that the complexes shown broader luminescence peaks, due to ligand metal charge transfer transitions LMCT [35].

Ligand, **HL** exhibited at 420nm as emission band and at 285 a.u. as intensity band, wherein the complexes observed considerable changes in the fluorescence characteristics due to moving longer wavelengths. The presence of bathochromic phenomenon shown from the emission bands for Co [1] (1), Ni[1] (2), Cu [1] (3), and Zn [1] (4) metal ions were observed at 365, 428, 432 and 497 nm with intensities of 798, 142, 136 and 156 a.u., respectively. This is due to resonant magnetic perturbation, electronic- energy transfer processes, redox activity etc., [36]. The fluorescence quenching intensity order for the complexes is Cu[1] > Ni[1] >Zn[1] > Co[1]. While Co[1] complex show less quenching because of chelation. Induced rigidity is main to cause change in fluorescent behaviour of free ligand on co-ordination to that of metal ion and is dependent on ligand's co-ordination geometry around metal centre. In the complexation process fluorescence enhancement that is of great interest as creates opportunity in photochemical applications for the complexes in further studies[35].

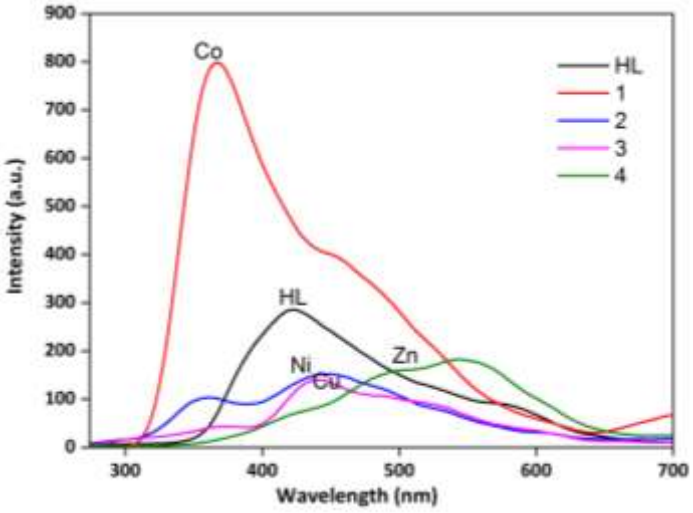

Figure 3. Photoluminescence spectra of Schiff base **HL** and its metal complexes (**1-4**) (2X 10^{-4} M)

3.1.4 NMR study

HL in DMSO solvent **Figure S1** was analysed for ^{1}H NMR spectrum and revealed a broad signal peak at 13.01 ppm, which corresponds to HBr. A singlet peak at 9.41 ppm (-OH) was ascribed to phenolic hydrogen at 8.78 ppm was attributed to azomethine hydrogen (7CH=N). A singlet 9.69 ppm was shown at 9.69 ppm for an isothiomide NH_2. The signals observed between 7.63 and 5.88 ppm were ascribed to aromatic hydrogens. The isothioallylic group (S-17CH_2) signals are found at 3.09 ppm[37].

^{13}C NMR spectroscopy, the 14C = N azomethine moiety of **HL** was observed at 163.2 ppm. The 7CH=N azomethine group was found at 149.9 ppm, which is a distinctive peak. In contrast, the carbon peaks of the 4C-OH, 3C-O-, and (S-17CH_2) isothioallyl groups correspond to 147.9, 147.5 and 34.1 ppm as shown in **Figure S2.** The ^{13}C NMR spectrum, carbon atoms of the aliphatic and aromatic groups lie within normal regions.

3.1.5 Mass study

The LC-MS ESI spectrum of Schiff base and its complex was recorded in acetonitrile solvent. The molecular formulae for **HL**, $C_{13}H_{18}BrN_3O_2S$ representative mass spectrum is shown in **Figure 1(a)**. The observed m/z = 280.11 $[M+H]^+$ (calcd. 279.10) as molecular ion peak. The base peak with the most stable component at *m/z* = 280 $[M+H]^+$ has been confirmed with other constituents. The other mass fragment peaks for HBr as $[M+H]^+$ were 302, 322 and 360. The **$[Zn(L)_2]^{2+}$** complex's mass spectrum was observed where the molecular ion peak for $C_{26}H_{32}N_6O_4S_2Zn$ at *m/z* = 621 $[M+H]^+$ (calcd. 620) is shown in **Figure 1(b).**

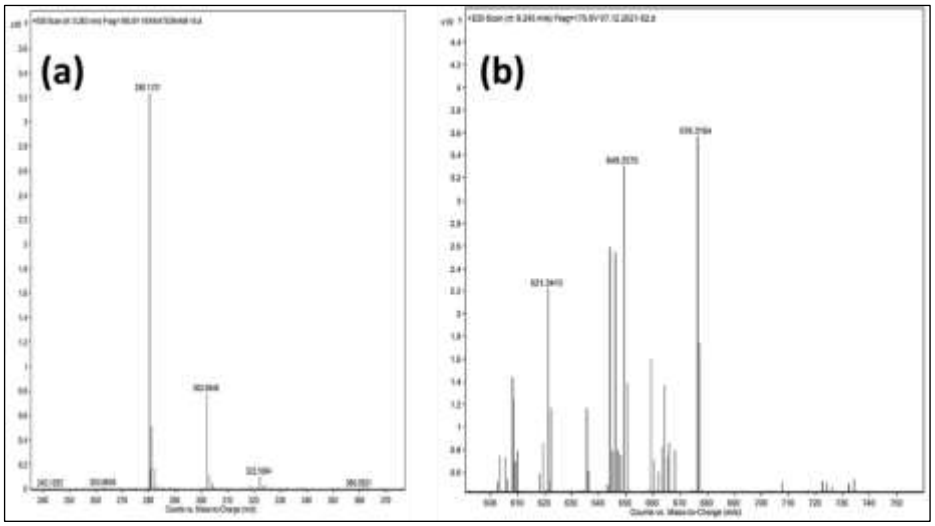

Figure 1. Mass spectrum of **HL (a)** and **$[Zn(L)_2]^{2+}$(b)**

3.1.6 ESR study

The polycrystalline state ESR spectrum of **$[Cu(L)_2]^{2+}$** was obtained at room temperature. ESR spectrum shown in **Figure 4** are gII = 2.23 > g⊥ = 2.06 > g_e = 2.0023 due to the reason that unpaired electron is mostly presented in the ground state 2B1g, which is predominantly located in the Cu[1] ions dx^2y^2 orbital, this suggests an octahedral geometry around copper ion. The gII value of metal complexes is an important factor that characterizes the bonding nature between metal ions and ligands [38]. The gII value was reported to be between 2.06-2.25, which is less than 2.3. Therefore, covalent metal-ligand bonding is tentatively proposed [22].

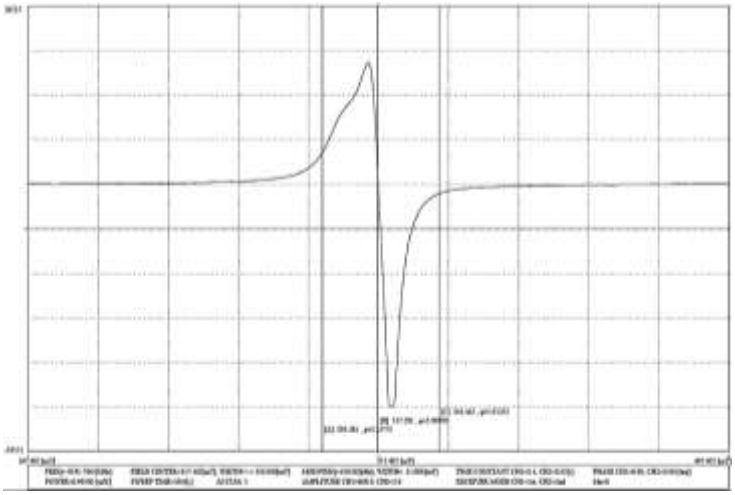

Figure 4. Polycrystalline ESR spectrum of $\mathbf{[Cu(L)_2]^{2+}}$

3.2 Biological activities

3.2.1 Antibacterial activity

Evaluations towards the **HL** and its complexes (**1-4**) anti-microbial activity tested were reported in supplementary material **Table S1**.

For these antibacterial properties, streptomycin was opted as positive control and standard, whereas as negative control DMSO. The Co [1], Ni [1], Cu [1] and Zn [1] complexes exhibits good action against a type of pathogen but substantially shown lower activity than that of standard, the ligand, **HL** was observed to be ineffective or weak against all pathogenic bacteria. Whereas, the complex $\mathbf{[Zn(L)_2]^{2+}}$ has very good activity against E. coli (27 mm), Salmonella paratyphi (25 mm), Bacillus subtilis (24 mm), and staphylococcus aureus (25 mm) strains. The remaining compounds antimicrobial activity order is Co[1] > Ni[1] > Cu[1] showed better to moderate activity against bacterial pathogen species. The bacterial order is Zn[1] > Ni[1] > Cu[1] > Co[1] > HL may be used to represent comparative efficiency that is based on overtone's concept and Tweey's Chelation theory [39], the increased the metal complexes' activities when compared to that of Schiff base ligands were explained[30, 40]. This theory permits the p-electron delocalization, along the entire chelate ring, that reduces metal ion positive charge and increases the metal chelates lipophilicity, which facilitates its passage via bacterial membran lipid layer [40-42].

3.2.2 In-vitro anti-diabetic activity

The alpha-amylase inhibition experiment was taken to explore the metal complexes anti-diabetic property in vitro. **Table 1** summarizes the findings. The Zn[1] chelating complex shown stronger anti-diabetic efficacy in the alpha-amylase assay. Within the limits of standard acarbose, all remaining metal complexes exhibited increasingly better activity than the free ligands. The best anti-diabetic action was found in the metal complex Zn[1]. The alpha-amylase inhibitory activity of **HL** and its complexes is found in the order HL< Ni[1] < Co[1] < Cu[1] < Zn[1]. The incorporation of metals may contribute to the improvement in the activity of complexes [41, 43, 44]. The complexes of Cu [1] and Zn [1] exhibited better activity than Co[1] and Ni[1] complexes. As an example, consider the following, according to scientific and clinical investigations, oxidative stress has a significant part in the pathophysiology and diabetes problem development[24].

Table 1. The alpha-amylase inhibitory activity of ligand and their complexes

Compounds	**IC_{50} (µM)**
HL	8.58 ± 0.65
$[Co(L)_2]$	9.54 ± 0.73

$[Ni(L)_2]$	4.28 ± 0.32
$[Cu(L)_2]$	28.37 ± 2.17
$[Zn(L)_2]$	29.53 ± 2.08
Acarbose (std)	33.17 ± 2.39

3.3 Molecular docking studies

In the current study to optimize the binding mechanism between the receptor and metal complexes, molecular docking studies were preferred. In this case, the mentioned compounds represent the ligands, whereas the receptor FabH-CoA complex of *E. coli* PDBID: 1HNJ protein. It is suggested that in order to test the antibacterial ability the FabH receptors are targeted of natural substances and also has a crucial involvement in Fatty acid bio-synthesis [22]. The results of molecular docking were reported in **Table 2**, **Figure 5** shows the good conformation position of the analyzed ligands in the 3D binding pocket. Several hydrogen bonds, electrostatic and hydrophobic interactions bind the relevant proteins to the 1HNJ pocket, resulting in considerable negative docking scores. This indicates a crucial interaction between the docked ligands and the active receptors. The ranking of the inhibitory activity of docked: Ni[1]) = Zn[1] > Cu[1] > Co[1] > HL. Finally, the studies explains that complexes $\mathbf{[Ni(L)_2]^{2+}}$ and $\mathbf{[Zn(L)_2]^{2+}}$ both have the most active binding energy (-6.5 kcal/mol) and are effectively attached to the ligands 1HNJ1 binding pocket through involvement of varying hydrogen bonds, electrostatic and hydrophobic interactions.

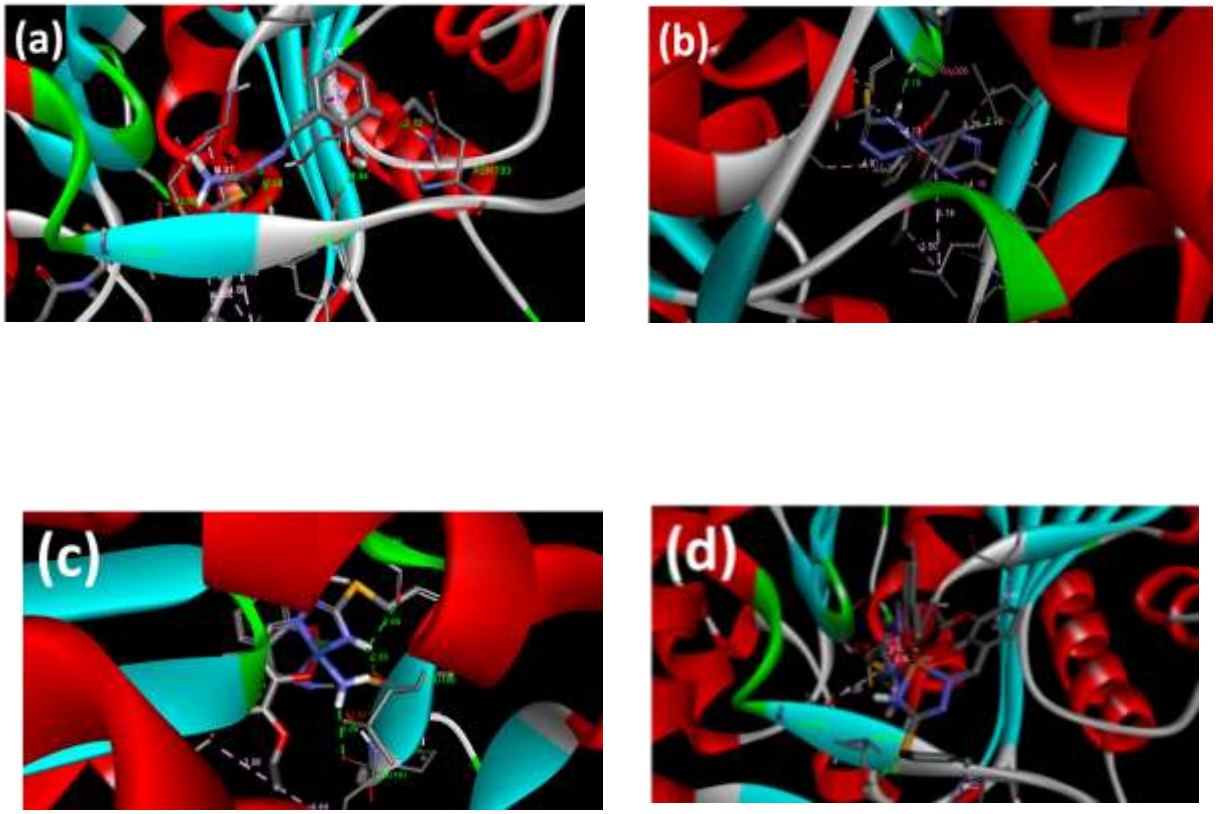

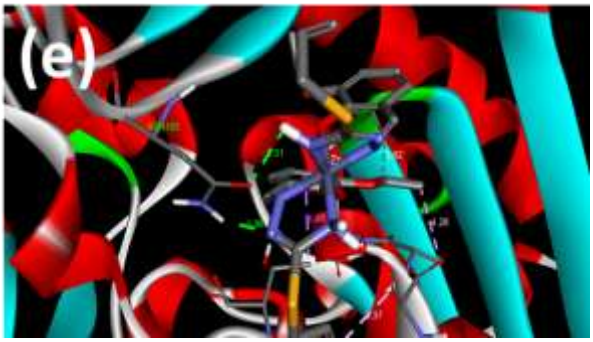

Figure 5. 3D docked lowest energy poses of ligand and its complexes with E. coli PDBID: 1HNJ protein targets of HL(**a**), $[Co(L)_2]$ (**b**), $[Ni(L)_2]$ (**c**), $[Cu(L)_2]$ (**d**) and $[Zn(L)_2]$ (**e**)

Table 2. Molecular docking parameters of ligands and its complexes against protein receptor *(PDB ID: (1HNJ)* on their docking score calculated by Autodock

Ligands	**Receptor atoms Acceptor group**	**Ligand atoms Donor**	**Hydrogen bonding Distance(Å)**	**Docking Score (kcal/mol)**
HL	OC-LEU 189	HO	2.50	-5.5
	HN-ASN 193	OC	2.12	
	OC-LEU 191	HO	2.44	
	HN-LEU 191	NC	2.56	
$[Co(L)_2]$	OC-GLY 306	HN	2.18	-6.1
$[Ni(L)_2]$	OC-GLY 186	HN	2.69	-6.5
	OC-LEU 191	HN	3.09	
	OC-LEU 189	HN	2.93	
$[Cu(L)_2]$	HO-THR 190	SC	2.41	-6.4
$[Zn(L)_2]$	OC-ASN 193	HN	2.31	-6.5
	HN-ASN 193	NC	1.96	

3.4 Drug-likeness studies

In order to assess the pharmacological potential, drug likeness metrics are determined. These characteristics have been estimated for a large number of compounds with known pharmacological properties, resulting in the formation of desired parameter ranges. The famous Lipinski's rule of five [58], according to this absorption and penetration are probably more as the molecular weight (MW) is less than 500, which is to be noted to ensure the novel drugs. The ADME characteristics of the compound, **HL** such as molecular weight (MW), HBA, HBD, MR, TPSA, BBB penetration, Bio-availability and log Kp are computed and listed in **Table S7**. According to the literature, the values of nHBA (number of Hydrogen bond acceptors) and nHBD (number of Hydrogen bond donors) has to be less than 10 and 5 correspondingly[45]. Its HBA and HBD values for **HL** are 4 and 2, respectively. The highest TPSA value is 140 $Å^2$ and for HL it is computed as 105.50 $Å^2$. MR is a value that ranges between 40 and 130. The ligand, **HL** has an MR value of 91.19. The high GI absorption side is reflected in **Table 3**, log Kp (Skin permeability) to be -5.95 and 0.55 as bio-availability [46] and a molecular weight (MW) of 360.27g/mol. According to the analogy above, ligand, **HL** possesses acceptable biological qualities with drug-like characteristics that should be investigated more in the future.

Table 3. ADME properties of ligand HL	
Molecular weight (MW)	360.27
Hydrogen Bond Donor (HBD)	2.00
Hydrogen bond acceptor (HBA)	4.00
Molar refractivity [47]	91.19
Topological polar surface area (TPSA $Å^2$)	105.50
Gastrointestinal (GI) absorption	High
Blood–brain barrier (BBB) penetration	No
Skin permeability (Log K_p(cm/s))	-5.95
Bio-availability	0.55

4 CONCLUSIONS

In the present work, 3-ethoxy-2-hydroxybenzaldehyde S-allylisothiosemicarbazone hydrobromide, **HL** ligand is chelating agent to generate Co [1], Ni [1], Cu [1], and Zn [1] complexes through ligand reactions with metal salts. The ligand, **HL** is bound through nitrogen of azomethine and isothioamide, phenolic hydroxyl. FT-IR, ^{1}H and ^{13}C-NMR, UV-Vis, fluorescence and ESR spectroscopic techniques were opted for investigating the compounds. Ligand, **HL** and its complexes are formed as $\mathbf{[M(L)_2]^{2+}}$ species as supported by mass spectrum of Zn[1] complex. These compounds showed better biological activity as that of the Standard drug streptomycin. In contrary, biological and molecular docking studies of $\mathbf{[Ni(L)_2]}$ and $\mathbf{[Zn(L)_2]}$ revealed that the compounds *in vitro* and *in silico* performed studies has moved well with antibacterial, molecular docking and antidiabetic abilities and ADME-drug like properties for ligand.

5. ACKNOWLEDGEMENT

The authors wish to gratefully thank Dr. P. Srinivas and Dayakar, Department of Biotechnology KU Warangal for carried out biological studies.

6. DISCLOSURE STATEMENT

No potential conflicts of interest were reported by the authors for this work.

7. FUNDING

This research did not receive a grant from governmental, private, or non-profit funding bodies.

8. REFERENCES

[1] M. Kaykhaii, M.R.J.C.R.i.A.C. Linford, Application of microextraction techniques including SPME and MESI to the thermal degradation of polymers: A review, 47(2) (2017) 172-186.

[2] Y.d. Kurt, B. Ülküseven, S. Tuna, M. Ergüven, S. Solakoğlu, Iron(III) and nickel(II) template complexes derived from benzophenone thiosemicarbazones, Journal of Coordination Chemistry 62(13) (2009) 2172-2181.

[3] Y.D. Kurt, B.J.J.o.C.C. Ülküseven, Unusual template condensation of benzophenone thiosemicarbazones and salicylaldehydes with nickel (II), 63(5) (2010) 828-836.

[4] M.S. Refat, I.M. El-Deen, Z.M. Anwer, S.J.J.o.C.C. El-Ghol, Spectroscopic studies and biological evaluation of some transition metal complexes of Schiff-base ligands derived from 5-arylazo-salicylaldehyde and thiosemicarbazide, 62(10) (2009) 1709-1718.

[5] V.M. Leovac, V. Divjaković, V.I. Češljević, R.J.J.o.t.S.C.S. Fazlić, Transition metal complexes with thiosemicarbazide-based ligand: Part 45-Synthesis, crystal and molecular structure of [2, 6-diacetylpyridine bis (S-methylisothiosemicarbazonato)] diazide-iron (III), 68(4-5) (2003) 425-433.

[6] R. Takjoo, J.T. Mague, A. Akbari, M.J.J.o.C.C. Ahmadi, Co (III) and Fe (III) complexes of Schiff bases derived from 2, 4-dihydroxybenzaldehyde S-allyl-isothiosemicarbazonehydrobromide, 66(22) (2013) 3915-3925.

[7] A. Akbari, H. Ghateazadeh, R. Takjoo, B. Sadeghi-Nejad, M. Mehrvar, J.T.J.J.o.M.S. Mague, Synthesis & crystal structures of four new biochemical active Ni (II) complexes of thiosemicarbazone and isothiosemicarbazone-based ligands: In vitro antimicrobial study, 1181 (2019) 287-294.

[8] R. Takjoo, A. Hashemzadeh, H.A. Rudbari, F.J.J.o.C.c. Nicolo, Copper (II) and molybdenum (VI) complexes with 5-bromosalicylaldehyde S-allylisothiosemicarbazone: Syntheses, characterizations and crystal structures, 66(2) (2013) 345-357.

[9] R. Takjoo, P. Ramasami, L. Rhyman, M. Ahmadi, H.A. Rudbari, G.J.J.o.M.S. Bruno, Structural and theoretical studies of iron (III) and copper (II) complexes of dianion N1, N4-bis (salicylidene)-S-alkyl-thiosemicarbazide, 1255 (2022) 132388.

[10] G. Balan, O. Burduniuc, I. Usataia, V. Graur, Y. Chumakov, P. Petrenko, V. Gudumac, A. Gulea, E.J.A.O.C. Pahontu, Novel 2-formylpyridine 4-allyl-S-methylisothiosemicarbazone and Zn (II), Cu (II), Ni (II) and Co (III) complexes: Synthesis, characterization, crystal structure, antioxidant, antimicrobial and antiproliferative activity, 34(3) (2020) e5423.

[11] G.A. Bogdanović, A. Spasojević-de Bire, V.M. Leovac, V.I.J.A.C.S.C.C.S.C. Češljević, Transition metal complexes with thiosemicarbazide-based ligands. XXXIX.[Benzoylacetone 3-methylisothiosemicarbazonato (2−)-O, N1, N4](pyridine-N) nickel (II), 55(10) (1999) 1656-1658.

[12] A. Fasihizad, A. Akbari, M. Ahmadi, M. Dusek, M.S. Henriques, M.J.P. Pojarova, Copper (II) and molybdenum (VI) complexes of a tridentate ONN donor isothiosemicarbazone: Synthesis, characterization, X-ray, TGA and DFT, 115 (2016) 297-305.

[13] H. Beraldo, D.J.M.r.i.m.c. Gambino, The wide pharmacological versatility of semicarbazones, thiosemicarba-zones and their metal complexes, 4(1) (2004) 31-39.

[14] A.P. Rebolledo, M. Vieites, D. Gambino, O.E. Piro, E.E. Castellano, C.L. Zani, E.M. Souza-Fagundes, L.R. Teixeira, A.A. Batista, H.J.J.o.i.b. Beraldo, Palladium (II) complexes of 2-benzoylpyridine-derived thiosemicarbazones: spectral characterization, structural studies and cytotoxic activity, 99(3) (2005) 698-706.

[15] Q. Wang, C. Bi, Y. Fan, X. Zhang, J. Zuo, S.J.R.J.o.C.C. Liu, A novel copper (II) complex with schiff base derived from o-vanillin and L-methionine: Syntheses and crystal structures, 37 (2011) 228-234.

[16] M. Braun, M. Mail, R. Heyse, W.J.S.o.T.T.E. Amelung, Plastic in compost: Prevalence and potential input into agricultural and horticultural soils, 760 (2021) 143335.

[17] L.H. Abdel-Rahman, A.M. Abu-Dief, H. Moustafa, S.K.J.A.O.C. Hamdan, Ni (II) and Cu (II) complexes with ONNO asymmetric tetradentate Schiff base ligand: synthesis, spectroscopic characterization, theoretical calculations, DNA interaction and antimicrobial studies, 31(2) (2017) e3555.

[18] L.H. Abdel-Rahman, N.M. Ismail, M. Ismael, A.M. Abu-Dief, E.A.-H.J.J.o.M.S. Ahmed, Synthesis, characterization, DFT calculations and biological studies of Mn (II), Fe (II), Co (II) and Cd (II) complexes based on a tetradentate ONNO donor Schiff base ligand, 1134 (2017) 851-862.

[19] B. Adalat, F. Rahim, M. Taha, S. Hayat, N. Iqbal, Z. Ali, S.A.A. Shah, A. Wadood, A.U. Rehman, K.M.J.J.o.M.S. Khan, Synthesis of Benzofuran–based Schiff bases as anti-diabetic compounds and their molecular docking studies, 1265 (2022) 133287.

[20] U. Salar, K.M. Khan, S. Chigurupati, S. Syed, S. Vijayabalan, A. Wadood, M. Riaz, M. Ghufran, S.J.M.C. Perveen, New hybrid scaffolds based on hydrazinyl thiazole substituted coumarin; as novel leads of dual potential; in vitro α-amylase inhibitory and antioxidant (DPPH and ABTS radical scavenging) activities, 15(1) (2019) 87-101.

[21] S.M. Hiremath, M.M. Basanagouda, S.S. Khemalapure, A. Rayar, A.M. Rakkasagi, V.V. Koppal, R. Mahesh, S.C.J.J.o.P. Jeyaseelan, P.A. Chemistry, Structural, vibrational, fluorescence spectral features, Hirshfeld surface analysis, docking and drug likeness studies on 4-(2-bromo-4-methyl-phenoxymethyl)-6-methyl-coumarin derivative: Experimental and theoretical studies, 431 (2022) 114055.

[22] A. Abdou, H.M. Mostafa, A.-M.M.J.I.C.A. Abdel-Mawgoud, Seven metal-based bi-dentate NO azocoumarine complexes: Synthesis, physicochemical properties, DFT calculations, drug-likeness, in vitro antimicrobial screening and molecular docking analysis, 539 (2022) 121043.

[23] S.K. Burley, H.M. Berman, C. Christie, J.M. Duarte, Z. Feng, J. Westbrook, J. Young, C.J.P.S. Zardecki, RCSB Protein Data Bank: Sustaining a living digital data resource that enables breakthroughs in scientific research and biomedical education, 27(1) (2018) 316-330.

[24] A. Kumar, D. Kumar, K. Kumari, Z. Mkhize, L.K. Seru, I. Bahadur, P.J.J.o.M.L. Singh, Metal-ligand complex formation between ferrous or ferric ion with syringic acid and their anti-oxidant and anti-microbial activities: DFT and molecular docking approach, 322 (2021) 114872.

[25] L.H. Abdel-Rahman, R.M. El-Khatib, L.A. Nassr, A.M.J.J.o.M.S. Abu-Dief, Synthesis, physicochemical studies, embryos toxicity and DNA interaction of some new Iron (II) Schiff base amino acid complexes, 1040 (2013) 9-18.

[26] V.M. Leovac, V.I. Češljević, N.J.P. Galešič, Transition metal complexes with the thiosemicarbazide-based ligands—V. Synthesis, crystal and molecular structure, and spectra of S-methyl-N (1)-salicylidene-N (4)-α-methoxypicolyl-isothiosemicarbazidonickel (II), 7(24) (1988) 2641-2647.

[27] D.-M. Xian, Z.-L. You, M. Zhang, P. Hou, X.-H.J.J.o.C.C. Li, Dinuclear Schiff-base copper (II) complexes with various bridging groups, 64(18) (2011) 3265-3272.

[28] M. Najar, C. Saldanha, K.J.I.j.o.n. Banday, Approach to urinary tract infections, 19(4) (2009) 129.

[29] A.Y. Genel, B. Ülküseven, İ.J.R.J.o.I.C. Kızılcıklı, Palladium (II) complexes of benzaldehyde and 2-hydroxybenzaldehyde-4-H/phenyl-S-ethyl/allyl-thiosemicarbazones, 53 (2008) 1747-1753.

[30] A. El-Sonbati, W. Mahmoud, G.G. Mohamed, M. Diab, S.M. Morgan, S.J.A.O.C. Abbas, Synthesis, characterization of Schiff base metal complexes and their biological investigation, 33(9) (2019) e5048.

[31] R. Takjoo, M. Hakimi, M. Seyyedin, M.J.J.o.S.C. Abrishami, New 2-pyridinealdehyde N 4-hydroxyethyl thiosemicarbazone and their Cd (II) and Cu (II) complexes: synthesis, spectral, in vitro antibacterial activity and molecular and supramolecular structure study, 31(5) (2010) 415-426.

[32] R. Takjoo, R. Centore, M. Hakimi, S.A. Beyramabadi, A.J.I.C.A. Morsali, S-allyl-3-(2-pyridyl-methylene) dithiocarbazate ligand and its manganese (II), cobalt (III) and nickel (II) complexes, 371(1) (2011) 36-41.

[33] B.I. Ceylan, Y.D. Kurt, B.J.J.o.C.C. Ülküseven, Synthesis and characterization of new dioxomolybdenum (VI) complexes derived from benzophenone-thiosemicarbazone (H2L). Crystal structure of [MoO2L (PrOH)], 62(5) (2009) 757-766.

[34] M. Keleş, T. Keleş, O.J.T.M.C. Serindağ, Palladium complexes with bis (diphenylphosphinomethyl) amino ligands and their application as catalysts for the Heck reaction, 33 (2008) 717-720.

[35] J. Devi, M. Yadav, D. Kumar, L. Naik, D.J.A.O.C. Jindal, Some divalent metal (II) complexes of salicylaldehyde-derived Schiff bases: Synthesis, spectroscopic characterization, antimicrobial and in vitro anticancer studies, 33(2) (2019) e4693.

[36] S. Konar, A. Jana, K. Das, S. Ray, S. Chatterjee, J.A. Golen, A.L. Rheingold, S.K.J.P. Kar, Synthesis, crystal structure, spectroscopic and photoluminescence studies of manganese (II), cobalt (II), cadmium (II), zinc (II) and copper (II) complexes with a pyrazole derived Schiff base ligand, 30(17) (2011) 2801-2808.

[37] Y.D. Kurt, B. Ülküseven, S. Güner, Y.J.T.M.C. Köseoğlu, Copper (II) and palladium (II) complexes of 2-amino-5-chlorobenzophenone and 2-(2-hydroxybenzylidene) amino-5-chlorobenzophenone-S-methyl-thiosemicarbazones, 32(4) (2007) 494-500.

[38] R. Konakanchi, G.S. Pamidimalla, J. Prashanth, T. Naveen, L.R.J.B. Kotha, Structural elucidation, theoretical investigation, biological screening and molecular docking studies of metal (II) complexes of NN donor ligand derived from 4-(2-aminopyridin-3-methylene) aminobenzoic acid, 34 (2021) 529-556.

[39] A. Ramesh, R. Pawar, P. Shyam, A.J.R.o.C.I. Ramachandraiah, Synthesis, DFT calculations and biological activity of a new Schiff base of 4-aminoantipyrine and its Co (II), Ni (II), Cu (II) and Zn (II) complexes and crystal structure of the Schiff base, 47 (2021) 4673-4697.

[40] T. Aiyelabola, J. Jordaan, D. Otto, E.J.A.i.B.C. Akinkunmi, Synthesis Characterization and Biological Activities of an Enamine Derivative and Its Coordination Compounds, 10(06) (2020) 172.

[41] A. Ramesh, B. Srinivas, R. Pawar, A.J.J.o.M.S. Ramachandraiah, Synthesis, characterization, crystal structure determination, computational modelling and biological studies of a new tetrakis-(2-hydroxy-5-methylphenyl)(1H-pyrazol-4-yl) methanonezinc (II) complex, 1255 (2022) 132377.

[42] A. Fekri, R.J.J.o.O.C. Zaky, Solvent-free synthesis and computational studies of transition metal complexes of the aceto-and thioaceto-acetanilide derivatives, 818 (2016) 15-27.

[43] D.M. Motloung, S.S. Mashele, G.R. Matowane, S.S. Swain, S.L. Bonnet, A.E. Noreljaleel, S.O. Oyedemi, C.I.J.J.o.P. Chukwuma, Pharmacology, Synthesis, characterization, antidiabetic and antioxidative evaluation of a novel Zn (II)-gallic acid complex with multi-facet activity, 72(10) (2020) 1412-1426.

[44] J.E. Philip, M. Shahid, M.P. Kurup, M.P.J.J.o.P. Velayudhan, P.B. Biology, Metal based biologically active compounds: design, synthesis, DNA binding and antidiabetic activity of 6-methyl-3-formyl chromone derived hydrazones and their metal (II) complexes, 175 (2017) 178-191.

[45] C.A. Lipinski, F. Lombardo, B.W. Dominy, P.J.J.A.d.d.r. Feeney, Experimental and computational approaches to estimate solubility and permeability in drug discovery and development settings, 23(1-3) (1997) 3-25.

[46] Y.C.J.J.o.m.c. Martin, A bioavailability score, 48(9) (2005) 3164-3170.

[47] R.B. Patel, M.J.P.R. Patel, An introduction to analytical method development for pharmaceutical formulations, 6(4) (2008) 1-5.